Peering towards Cosmic Dawn
Proceedings IAU Symposium No. 333, 2018
V. Jelić & T. van der Hulst, eds.

doi:10.1017/S1743921317011152

Foreground mitigation strategy for measuring the 21 cm-LAE cross-correlation†

Shintaro Yoshiura[1], Jack L. B. Line[2,3], Kenji Kubota[1], Kenji Hasegawa[4] and Keitaro Takahashi[1]

[1]Department of Physics, Kumamoto University, Kumamoto,Japan
email: 161d9002@st.kumamoto-u.ac.jp
[2]The University of Melbourne, Melbourne, Australia
[3]ARC Centre of Excellence for All-sky Astrophysics (CAASTRO)
[4]Department of Physics, Nagoya University, Aichi , Japan

Abstract. The cross power spectrum of the 21 cm signal and Lyman-α emitters (LAEs) is a probe of the Epoch of Reionization. Astrophysical foregrounds do not correlate with the LAE distribution, though the foregrounds contribute to the error. To study the impact of foregrounds on the measurement, we assume realistic observation by the Murchison Widefield Array using a catalogue of radio galaxies, a LAE survey by the Subaru Hyper Supreme-Cam and the redshift of LAEs is determined by the Prime Focus Spectrograph. The HI distribution is estimated from a radiative transfer simulation with models based on results of radiation hydrodynamics simulation. Using these models, we found that the error of cross power spectrum is dominated by foreground terms. Furthermore, we estimate the effects of foreground removal, and find 99% of the foreground removal is required to detect the 21 cm-LAE signal at $k \sim 0.4\,h\,\mathrm{Mpc}^{-1}$.

Keywords. cosmology: observations

1. Introduction

After the cosmic recombination, the IGM is rich in neutral hydrogen (HI). During the epoch of reionization (EoR), the HI gases are ionized by photons emitted from first stars and galaxies. Although the EoR has been explored, there is no crucial observation for the nature of the main sources of reionization and global history of the HI fraction. The redshifted 21 cm signal emitted from HI gas is expected to be an useful tool for revealing them. However, bright foregrounds, such as the galactic synchrotron emission and radio loud galaxies, are a few orders of magnitude brighter than the faint 21 cm signal. Thus, the foregrounds have to be removed precisely. However, perfect modeling of the foregrounds is impossible because no instrument can detect all point sources. Furthermore, instrumental and calibration errors make the foreground removal complicated.

To reduce the foreground contamination, the cross correlation with other observables is useful. In this work, we focus on the cross-correlation between the 21 cm signal and Lyman-α emitters (LAEs). LAEs are high-z galaxies and candidates of the main ionizing sources during the EoR. When a LAE makes an ionized bubble around itself, the 21 cm signal is zero from the region. Therefore, the distribution of LAEs anti-correlates with the 21 cm signal. On the other hand, LAEs are not strongly correlated with foreground sources, and the cross power spectrum of foregrounds and LAEs should be zero. In many

† To appear in the proceedings of "Peering towards Cosmic Dawn" (IAU Symposium 333, 2nd-6th October 2017, Dubrovnik, Croatia). This presentation is based on the paper Yoshiura *et al.* (2017) accepted to MNRAS.

previous works, the cross correlation and detectability are investigated (e.g. Lidz *et al.* (2009), Park *et al.* (2014), Kubota *et al.* (2017)).

Previous studies of the 21 cm-LAE correlation show that the signal will be observed by the radio interferometers such as the Murchison Widefield Array (MWA, Tingay *et al.* (2013), Bowman *et al.* (2013)) and the low frequency Square Kilometre Array (SKA_LOW, Mellema *et al.* (2013)). However, these studies assume the foreground sources have no effects on feasibility. However, even if the LAE distribution has no correlation with the foregrounds, the foregrounds produce statistical variance which contributes to the error of the 21 cm-LAE cross power spectrum. Moreover, the foregrounds can be strongest error since the power spectrum is much brighter than the 21 cm signal. Thus, the quantitative estimation of the foreground contamination is instructive for future observations. To predict the feasibility, we use a numerical simulation of reionization, and foreground models based on recent observation and realistic instrumental effects.

2. Method

Although the LAE has no correlation with the foregrounds, the foregrounds add variance to the 21 cm-LAE signal. The error on the signal is estimated as $\sigma^2 \propto P_{21,\mathrm{LAE}} + (P_{21} + P_{\mathrm{FG}} + N_{21})(P_{\mathrm{LAE}} + N_{\mathrm{LAE}})$, where $P_{21,\mathrm{LAE}}$ is the 21 cm-LAE cross power spectrum, P_{21}, P_{FG} and P_{LAE} are the auto power spectrum of the 21 cm signal, foregrounds and the LAE number density. N_{21} is the thermal noise term of the 21 cm observation and N_{LAE} is the shot noise of the LAE survey.

To estimate the error of the 21 cm-LAE cross power spectrum, we calculate these power spectrums from our models. To obtain an uv coverage of visibility which is crucial to estimate the foreground contribution, we simulate an MWA observation with an actual tile distribution and a beam model. For the extragalactic point sources, we build a model based on the GLEAM catalogue (Hurley-Walker *et al.* (2017)). We also combine a parametric model of Galactic diffuse emission and the visibility distribution (Jelić *et al.* (2008)). The power spectrum of the foreground is estimated from visibilities by following Thyagarajan *et al.* (2013). Furthermore, the thermal noise is also estimated from the visibility distribution of the MWA with 128 tiles, and 1000 hours is assumed as total observation time.

The 21 cm brightness temperature distribution is calculated using a large scale cosmological simulation. In the numerical simulation, we solve post processed radiative transfer (RT) with models based on an RHD simulation. According to the result of RHD simulation, the clumping factor and the escape fraction of galaxies depend on matter density, ionized fraction and halo mass. The matter density is obtained by using an N-body simulation performed with GreeM (Ishiyama *et al.* (2009)) which is a massive parallel TreePM code. In this proceedings, we employ 'late' model for estimating the 21 cm signal. This model has 6.7mK as averaged 21 cm brightness temperature and 0.44 as volume averaged neutral fraction. For more details of this model, please see Kubota *et al.* (2017).

To identify LAEs, we use a Lyman-α transmission code (Yajima *et al.* (2017)). The parameters of LAEs are chosen so that the luminosity function of LAE is consistent with observation (Konno *et al.* (2017)). We also assume the redshift of LAEs is identified by the PFS spectroscopic observation with tiny redshift error ($\Delta z = 0.0007$).

3. Foreground Contamination & Forecast

In the Fig. 1, we compare the 21 cm-LAE signal and error in the 2D plane. The $k_\perp$ is k-mode in the plane of the sky, and $k_\parallel$ is derived from the frequency which is the scale

https://doi.org/10.1017/S1743921317011152 Published online by Cambridge University Press

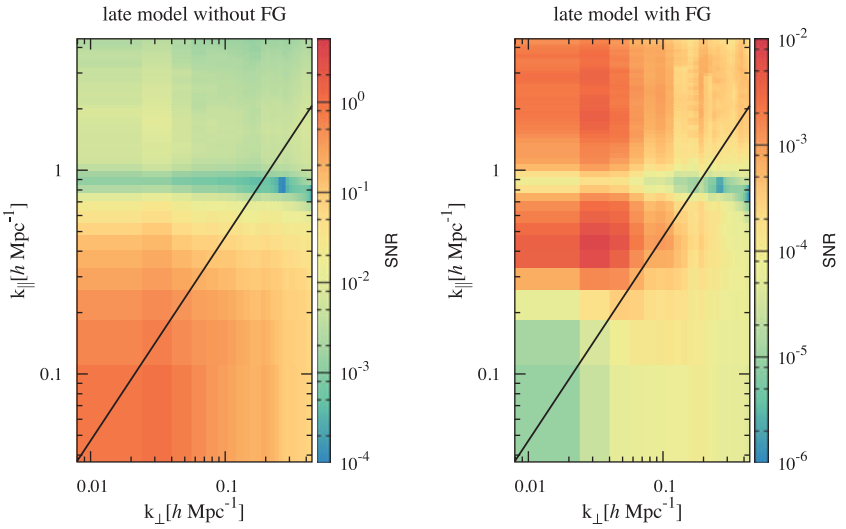

Figure 1. The signal to noise ratio (SNR) in the 2D power spectrum. In the left panel, we ignore the foreground error. In the right panel, foregrounds are included in error. The expected foreground contamination of point sources is shown as the solid line.

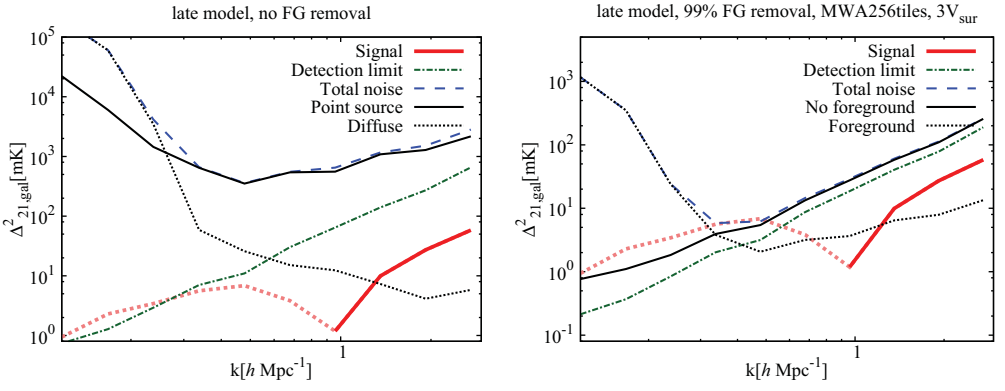

Figure 2. The comparison between the expected signal and the expected error. The thick line shows 21 cm-LAE signal and the sign is negative at large scales, indicated by the dotted line. The positive part is solid. The dashed line is the total expected error. The dot-dashed line shows the error term of thermal noise and shot noise. For the left panel, no foreground removal is applied. The thin solid and thin dotted lines show error of the point source and diffuse emission respectively. For the right panel, we subtract 99% of all foregrounds and assume 256 tiles of MWA and 3 times larger LAE survey area. The thin dotted lines shows the error of foregrounds and the thin solid line shows the contribution from other terms.

of our line of sight direction. In the left panel, we ignore the foreground contamination to estimate the intrinsic signal to noise ratio (SNR). The structure of SNR is the same as the 21 cm-LAE signal, and the signal is detectable on large scales. We note that the signal is negative at large scales and positive at small scales. The horizontal stripe seen at $k_{\parallel} = 0.9\,h\,\mathrm{Mpc}^{-1}$ indicates the sign transition. The right panel shows the SNR with the error term of foregrounds added. At large scales, the SNR is reduced to 10^{-4} because the foreground dominates. In the top left conner of 2D plane, so-called 'EoR window', the foreground contribution is small, and the SNR is about 0.01.

https://doi.org/10.1017/S1743921317011152 Published online by Cambridge University Press

The error including the foregrounds can be reduced by spherically averaging in a 2D plane. In Fig. 2, we show the 1D power spectrum calculated from the 2D power spectrum. In the left panel, the contribution from point source and diffuse emission are shown as thin solid and dotted lines. The detection limit is set by thermal noise and shot noise. The signal is shown as thick line and it is larger than the detection limit at large scales. Thus, if the foregrounds do not contribute to error, there is a possibility of measurement. However, the total error is a few orders of magnitude larger than the expected signal. Thus, precise foreground removal is required to measure the 21 cm-LAE signal. At small scales, higher sensitivity is also required for the detection.

In the right panel of Fig. 2, we demonstrate the error after removing foregrounds. We assume 99% foreground removal and the 21 cm-line observation with 256 MWA tiles. Thus, we reduce the thermal noise and the foreground power spectrum by factors of 4 and 10^4 at all scales. In addition, we increase the survey area of the HSC survey by a factor of 3. As shown in the panel, the 21 cm-LAE signal is consistent with total error at $k = 0.4\,h\,\mathrm{Mpc}^{-1}$. At large scales, $k < 0.4\,h\,\mathrm{Mpc}^{-1}$, the error is dominated by foreground contribution. Thus, more precise foreground removal is required to detect the scales. On the other hand, at small scales, $k > 0.4\,h\,\mathrm{Mpc}^{-1}$, the thermal noise term dominates the error. Therefore, future interferometers with high sensitivity such as MWA phase 2 and SKA_LOW should be able to detect the positive correlation.

Acknowledgement

This work is supported by Grant-in-Aid from the Ministry of Education, Culture, Sports, Science and Technology (MEXT) of Japan, No. 16J01585 (SY)., No. 26610048 (KT), No.15H05896 (KT), No.16H05999 (KT), No.17H01110 (KT), and Bilateral Joint Research Projects of JSPS (KT).

References

Bowman, J. D., Cairns, I., Kaplan, D. L., *et al.* 2013, *PASA*, 30, e031
Furlanetto, S. R. & Lidz, A. 2007, *ApJ*, 660, 1030
Hurley-Walker, N., Callingham, J. R., Hancock, P. J., *et al.* 2017, *MNRAS*, 464, 1146
Ishiyama, T., Fukushige, T., & Makino, J. 2009, *PASJ*, 61, 1319
Jelić, V., Zaroubi, S., Labropoulos, P., *et al.* 2008, *MNRAS*, 389, 1319
Konno, A., Ouchi, M., Shibuya, T., *et al.* 2017, arXiv:1705.01222
Kubota, K., Yoshiura, S., Takahashi, K., *et al.* 2017, arXiv:1708.06291
Lidz, A., Zahn, O., Furlanetto, S. R., *et al.* 2009, *APJ*, 690, 252
Mellema, G., Koopmans, L. V. E., Abdalla, F. A., *et al.* 2013, *Experimental Astronomy*, 36, 235
Park, J., Kim, H.-S., Wyithe, J. S. B., & Lacey, C. G. 2014, *MNRAS*, 438, 2474
Thyagarajan, N., Udaya Shankar, N., Subrahmanyan, R., *et al.* 2013, *APJ*, 776, 6
Tingay, S. J., Goeke, R., Bowman, J. D., *et al.* 2013, *PASA*, 30, e007
Yajima, H., Sugimura, K., & Hasegawa, K. 2017, arXiv:1701.05571
Yoshiura, S., Line, J. L. B., Kubota, K., Hasegawa, K., & Takahashi, K. 2018, accepted to MNRAS